THE FRACTAL NATURE OF THE ELECTROMAGNETIC FIELD WITHIN A REVERBERATING CHAMBER

A. Sorrentino*, L. Mascolo, G. Ferrara, and M. Migliaccio

Dipartimento per le Tecnologie, Università degli Studi di Napoli Parthenope, Centro Direzionale, Isola C4, Naples, Italy

Abstract—In this paper, a new look at the electromagnetic field in a reverberating chamber (RC) is presented. It follows the fractional Brownian motion (fBm) model and exploits the Hurst parameter as the key parameter to discriminate among various RC configurations. Experiments accomplished at the RC of the Università di Napoli Parthenope, formerly Istituto Universitario Navale (IUN), confirm the physical soundness of the proposed model.

1. INTRODUCTION

Reverberating Chamber (RC) enjoys growing popularity as a very attractive emulator of real-life environments. Hence, the RC first used only as high field amplitude test facility for electromagnetic interference (EMI) and compatibility (EMC), is now currently used for a wide range of other measurements and applications, which include, but are not limited, to radiated emission, shielding characterization of material, antenna efficiency, exposition of biological material. Moreover, since wireless applications have gained more and more importance, the RC has attracted some interest as a repeatable test facility where the devices and the communications can be tested.

The RC is an electrically large metallic enclosure in which the input electromagnetic field is properly randomized by means of an appropriately tailored process. The general principle of this randomization is the generation of a statistically distributed field, uniform, isotropic and randomly polarized.

In order to emulate and analyze the field in a RC appropriate models and procedures have been conceived and applied [1–10].

In [1, 2] the well-established mode theory is proposed. By means of the modal analysis it is shown that the amplitude of the RC electric field is Rayleigh distributed. The main drawback in the employment of the mode theory for RC description lies in the not convenient use for predicting the response of the reference antenna or the test object in the chamber environment.

In [3, 4] the plane wave integral representation of the field, that satisfies Maxwell's equations and also include the statistical properties expected for a well-stirred field, is presented. The statistical nature of the field is introduced through the statistical properties of the plane wave coefficients. In this way, it is simple to use it to calculate the responses of the test object or reference antenna.

Last but not least, the RC field has been described in terms of replicas of the transmitting field with proper polarization, phase and time delay that are superimposed at the receiver side [5–8]. When only scattered waves arrive at the terminal, the chamber emulates a NLOS propagation channel [5–7]. Differently, when also a direct link between the receiver and the transmitter antenna is present, a LOS propagation channel occurs [8–10].

An alternative description of the RC field is given in terms of chaotic model. The chaotic behavior of a mode-stirred RC is illustrated in [11, 12]. In [11] the chaotic properties of the RC field are gauged in terms of Lyapunov exponent. Orjubin in [12] presents a study of the chaoticity of an RC through the statistic of the eigen-frequencies that are numerically determined by Finite Elements Method (FEM). In both papers the chaotic behavior is numerically assessed but no experimental results is provided to validate the theoretical model.

In this paper, the fractal model based on the fractional Brownian motion (fBm) is used and tested over real measurements.

The fBm model is a physically grounded tool to look for alternative RC parameter descriptors and estimators that could enhance the comprehension of the RC electromagnetic fields.

Conceptually, this model can be framed within the chaotic approach although the specific model that is used here is new. Further, for the first time, a test on real experimental measurements of a chaotic model is done.

2. THE fBm MODEL OF THE ELECTROMAGNETIC FIELD IN THE RC

In this section, the fBm model, used in this paper, is described and discussed. From chaos theory, a chaotic system is defined as a dynamical system that exhibits a random-like behavior. When such

behavior occurs, the system is said to possess a strange attractor and the system itself is said to be chaotic [13]. Since strange attractors are fractal sets [13], chaotic systems, such as the electromagnetic field in an RC, can be therefore studied by means of the fractal theory.

The electromagnetic field received by a linearly polarized receiving antenna is random and can be written as the sum of a large number, say N, of elementary scattered fields [14]. By using the complex phasor representation, the phasor at time t is given by

$$\hat{E}(t) = \sum_{n=1}^{N} a_n(t)e^{-j\Phi n(t)}, \tag{1}$$

where the factors $a_n(t)$ and $\Phi_n(t)$ are random variables which represent the amplitude and the phase associated to the n-th elementary field. This model well matches the NLOS behavior of the electromagnetic field in a RC [5, 6].

Mathematically, (1) can be seen as a random walk in a complex plane in which the number of steps is ruled by N [14]. By sampling the field at uniform time step τ we can construct the sequence $\left\{\hat{E}_m\right\} = \left\{\hat{E}_1, \hat{E}_2, \ldots, \hat{E}_M\right\}$ where $\hat{E}_m = \hat{E}(t = t_m = m\tau)$, with m spanning from 1 to M. This sequence is a set of complex and stationary Gaussian random variables, and hence the m-th sample can be expressed as

$$\hat{E}_m = E_m^{\text{re}} + jE_m^{\text{im}}, \tag{2}$$

where j is the imaginary unit and E_m^{re} and E_m^{im} are the real and the imaginary part of the received field. These latter are both Gaussians and stationary random variables.

Without loss in generality let us now to consider only the real part of (2). It is possible to define the function $B_H^{\text{re}}(\cdot)$ as the cumulative sum of the field samples [15]

$$B_H^{\text{re}}(t_m) = \sum_{l=1}^{m} E_l^{\text{re}}. \tag{3}$$

A sequence $B_H^{\text{re}}(\cdot)$ of values can be obtained by spanning from $m = 1$ to M.

From (3), each sample can be written in terms of the function $B_H^{\text{re}}(\cdot)$ as follows

$$\begin{aligned} E_1^{\text{re}} &= B_H^{\text{re}}(t_1) \\ E_m^{\text{re}} &= B_H^{\text{re}}(t_m) - B_H^{\text{re}}(t_{m-1}), \quad \forall m > 1. \end{aligned} \tag{4}$$

Eq. (4) shows that since the field sequence is a set of Gaussian variable, the time difference of $B_H^{\text{re}}(\cdot)$ values, also knows as increments, are

Gaussian and stationary. This suggests that the function $B_H^{re}(\cdot)$ is a fBm [15], with H being the Hurst parameter, which can assume any value in the range $0 < H < 1$ [15].

In summary, the fBm of parameter H is defined to be a random process on some probability space such that for any $t \geq 0$ ad $\tau > 0$ the increment $\{B_H(t+\tau) - B_H(t)\}$ has the normal distribution with zero mean and variance τ^{2H} [15].

When $H = 1/2$, the correlation between the past and the future increments of $B_H^{re}(\cdot)$ vanishes [15] and the special case of a Brownian motion [15], with independent, stationary and normally distributed increments, is obtained [15]. In terms of RC field, this corresponds to the ideal case of a perfectly well stirred chamber which gives rise to a completely randomized field, i.e., with independent field samples.

Cases where $H \neq 1/2$ are properly fractional [15], and the correlation between the fBm increments is not zero [15], that is, the variation of the chamber geometry with time gives rise to a correlated field. In particular, two families of fBm's corresponding respectively to $H > 1/2$ and $H < 1/2$, can be defined. The first one corresponds to a positive correlation between the increments of $B_H^{re}(\cdot)$. In such a case the fBm is said to be persistent [15]. For $H < 1/2$, the correlation is negative, leading to an antipersistent fBm [15].

For the purpose of this paper, the most important fBm property is the spectral behavior. The fBm is a non-stationary random process [16] and therefore, its power spectrum cannot be defined by means of the Wiener-Khinchin theorem. Nevertheless, the power spectral density (PSD) of a fBm, i.e., the square of the absolute value of its Fourier Transform (FT), is given by [16]

$$S_{B_H}(\omega) = \frac{1}{\omega^\beta} \qquad (5)$$

where $\beta = 2H + 1$. It must be pointed out that the evaluation of β is a main step for the estimation of the Hurst parameter. If one uses the logarithmic scale, (5) can be rewritten as follows

$$\log_{10}\left(S_{B_H}(\omega)\right) = -\beta \log_{10}(\omega). \qquad (6)$$

Eq. (6) is a linear relationship in a logarithmic plane. Therefore, by means of a linear regression, for instance the Least Mean Square method (LMS), we can get β and H

$$H = \frac{\beta - 1}{2}. \qquad (7)$$

It is important to note that in real case the fractal model must be meant as physical fBm model, i.e., band-limited fractal.

Coming back to the complex field model we note that in our NLOS RC case $B_H^{re}(\cdot)$ and $B_H^{im}(\cdot)$, where $B_H^{im}(\cdot)$ is the fBm of the imaginary

part, are two independent fBm's having the same Hurst parameter. Therefore, the function

$$B_H(t_m) = B_H^{\text{re}}(t_m) + jB_H^{\text{im}}(t_m) \tag{8}$$

is an fBm in the complex plane [17], whose increments are normally distributed, stationary and with the correlation depending on the H values [16].

3. EXPERIMENTS: PRESENTATION AND DISCUSSION

This sections presents and discusses some experiments in support of the fractal theory detailed in Section 2. The data analyzed are measured at the IUN RC. It is a 2 m size cubic aluminum chamber whose internal walls and in which three stirrers are used to randomize the field. The first one (S1) is on the left of the entrance door, its shape is rectangular of about $1.84\,\text{m} \times 0.45\,\text{m}$ size; the second stirrer (S2) is in front of the entrance door and its shape is approximately a Greek cross whose bars are about of $1.84\,\text{m} \times 0.25\,\text{m}$ size; the third stirrer (S3) is located on the top of the chamber and is similar to S2 but for bars size which are about of $1.20\,\text{m} \times 0.18\,\text{m}$.

The three stirrers can rotate at 190 rpm, 320 rpm and 390 rpm, respectively. The transmitting and receiving antennas are both Ets-Lindgren double-ridged waveguide horn certified to work in the 1–18 GHz frequency range.

In all the experiments an Agilent Technologies Vector Network Analyzer (VNA) is used to transmit and to receive monochromatic signals: 16001 samples over a 3.6 s period are acquired at a sampling rate of 0.224 ms. The operating frequency used in these measurements is 10 GHz. A full calibration of the system is *a priori* undertaken. The complex scattering coefficient S_{21} is measured and an off-line data analysis is accomplished.

In this study, the key parameter that is evaluated is the Hurst parameter, associated to the fBm model of the field (Section 2).

Since the number of available data samples is large enough, a consistent estimator of the fBm spectrum is the averaged periodogram [18]. Data have been divided in $L = 8$ blocks, i.e., 2000 samples for each block. The spectrum evaluated for each block is averaged on the total number of spectra obtained. In such a way, the mean is the same and the variance is will be decreased by a factor of L. In Fig. 1 a sketch of the measurement setup is shown.

In the first set of measurements, the stirrers S1, S2, S3 are all operated. The transmitting and receiving antennas are cross-polarized and not faced to each other. The transmitting antenna is placed on

the left side of the chamber, faced to the corner close to the entrance door. The receiving antenna is faced to S2 stirrer (see Fig. 1 position a and b respectively). The complex fBm corresponding to this case is shown in Fig. 2. The real and the imaginary part of this process are two independent real valued fBm's, and therefore they satisfy the self-affinity condition [16]. The auto-affinity property can be applied to the data only when the estimation of H is provided. Let us determine H.
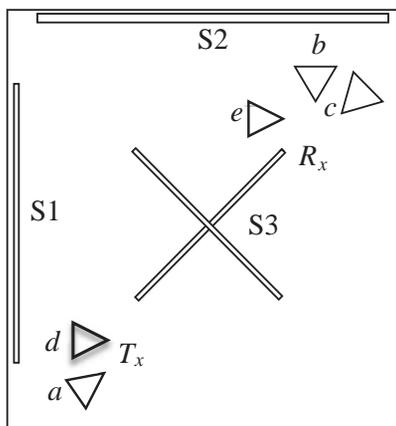
Figure 1. Schematic top view of he IUN RC.
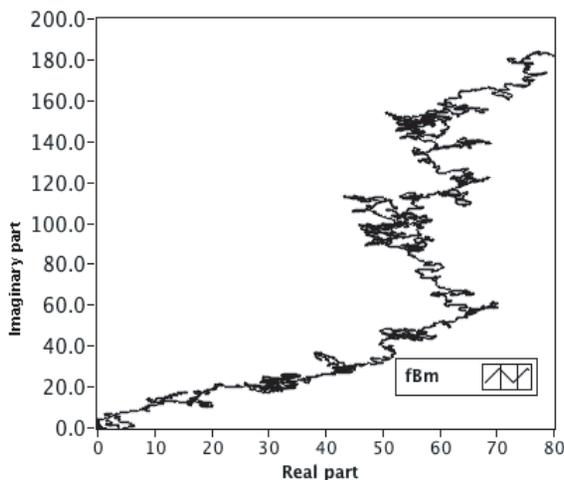
Figure 2. fBm associated to completely randomized field samples.
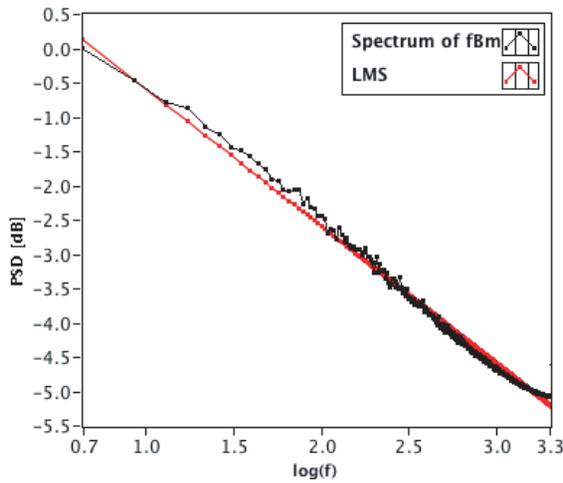
Figure 3. One-sided spectrum of the fBm (black line) and LMS fitting line (red line) in a bi-logarithmic plane, in the case of uncorrelated field samples. The operating frequency is 10 GHz.

Table 1. Values of H for different frequencies and different stirrer working configurations.

RC Configuration	H values	LMS error
S1, S2, S3 operated (Case I, 10 GHz)	0.504	4.72×10^{-4}
S1, S2, S3 operated (Case II, 10 GHz)	0.506	4.47×10^{-4}
S1, S2, S3 operated (1.8 GHz)	0.510	6.34×10^{-4}
S1 operated at 190 rpm (10 GHz)	0.471	3.13×10^{-4}
S1 operated at 22 rpm (10 GHz)	0.462	2.97×10^{-4}
S1 operated at 190 rpm (1.8 GHz)	0.463	5.07×10^{-4}
S1 operated at 22 rpm (1.8 GHz)	0.455	4.90×10^{-4}

The PSD of the fBm is shown in Fig. 3. It is important to note that experimental results shown in this paper are all relative to an operating frequency equal to 10 GHz. Measurements at different frequencies (not shown to save space) have been also accomplished, see Table 1.

In order to obtain an estimation of β, the data points in the logarithmic plane are modeled by a linear regression by applying the LMS method. Fig. 3 shows the one-side spectrum of the fBm in a bi-logarithm plane (black line) and the linear regression which

corresponds to the related LMS estimation (red line). It is important to note that the one-side spectrum has been normalized to the maximum value. The good agreement of the LMS estimation is confirmed by the fitting error In this case, the error in the fitting is $\varepsilon = 4.72 \times 10^{-4}$. Therefore, the good agreement between the spectrum and the LMS linear regression confirms the physical soundness of describing the RC field in terms of fBm, since the power spectrum of its cumulative sum follows a power-law decaying. The LMS estimation results in a value of β equal to 2.008 which corresponds to the Hurst parameter $H = 0.504$. Such a result indicates that the fBm increments, that is, the received field samples, are uncorrelated and hence statistically independent. The autocorrelation function (ACF, not shown to save space) confirms the behavior of the RC field.

To further validate the obtained results, experiment on a new set of data has been considered. It is important to point out that the chamber configuration is the same of the previous experiment, but for the receiving antenna in position c. The Hurst parameter is equal to $H = 0.506$, that means the samples are uncorrelated and statistically independent. Fig. 4 shows the spectrum of the fBm corresponding to the second set of measurements. In such a case, the evaluation of the error of LMS provides $\varepsilon = 4.47 \times 10^{-4}$ confirming again the good agreements between the two curves. Values of experimental results are
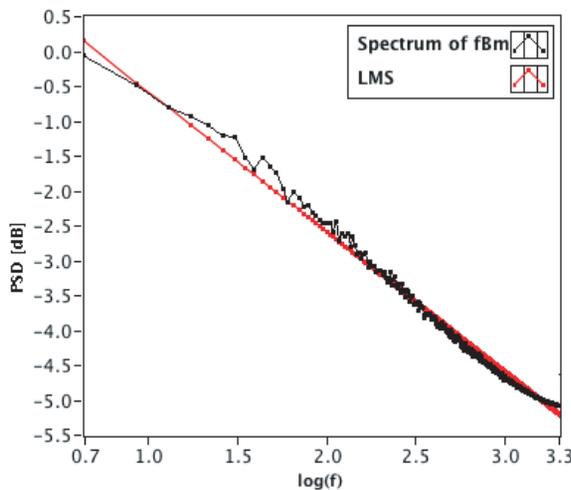
Figure 4. One-side spectrum of the fBm (black line) and LMS line (red line) in a bi-logarithmic plane for the second set of uncorrelated field samples. The operating frequency is 10 GHz.
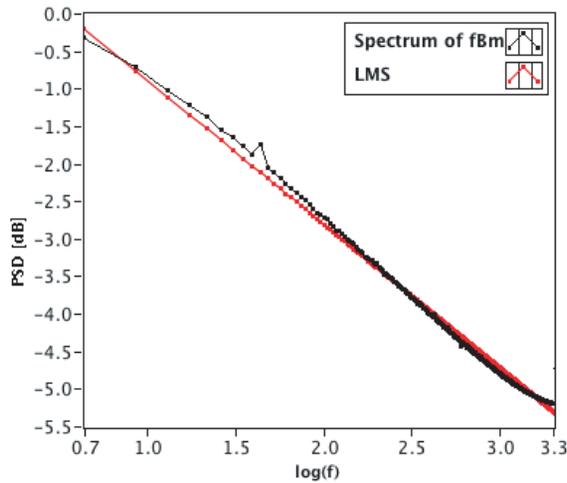
Figure 5. One-sided spectrum of the fBm (black line) and LMS fitting line (red line) in a bi-logarithmic plane in the case of correlated field samples. The operating frequency is 10 GHz.

listed in Table 1.

In order to change the correlation in the RC field [6], measurements with only the S1 stirrer working have been accomplished. The S1 stirrer has operated at different rates. The transmitting and the receiving antenna are both faced to S1 (see Fig. 1, position d and e respectively). The average periodogram has been determined and then, the LMS method provided the estimation of H. Results are listed in Table 1. The error introduced by the LMS fitting and the agreement between the value of H and the ACF of the field, in each case, confirm the physical soundness of the proposed model. In particular, Fig. 5 shows the spectrum obtained in the case of correlated samples when the S1 stirrer is moved to 190 rpm. The H value, in this case, is equal to 0.462, as listed in Table 1.

4. CONCLUSIONS

A fractal-based model to characterize the field in a reverberating chamber has been presented, discussed, and validated by a set of experiments conducted at the IUN RC. It has been shown that the fractal analysis of the field within the chamber, in terms of fBm, turns out to be tailored as an alternative description of the field in the RC. As matter of fact, it must be pointed out that:

– The spectrum of the cumulative sum of the RC field samples follows a power-law behavior, in agreement with the spectrum of the fBm process.

– Accordingly, the electromagnetic field within the RC can be characterized by the Hurst parameter, which represents a synthetic indicator to describe the first and second order statistical property of the field.

ACKNOWLEDGMENT

REFERENCES

1. Liu, B. H., D. C. Chang, and M. T. Ma, "Eigenmodes and the composite quality factor of a reverberating chamber," U.S. Nat. Bur. Stand. Tech. Note 1066, 1983.

2. Lehman, T. H., "A statistical theory of electromagnetic fields in complex cavities," *Interaction Notes*, Note 494, 1993.

3. Hill, D. A., "Plane wave integral representation for fields in reverberation chamber," *IEEE Trans. Electromagn. Compat.*, Vol. 40, No. 3, 209–217, 1998.

4. Hill, D. A. and J. Ladbury, "Spatial-correlation functions of fields and energy density in a reverberation chamber," *IEEE Trans. Electromagn. Compat.*, Vol. 44, No. 1, 95–101, 2002.

5. Ferrara, G., M. Migliaccio, and A. Sorrentino, "Characterization of GSM non-line-of-sight propagation channels generated in a reverberating chamber by using bit error rates," *IEEE Trans. Electromagn. Compat.*, Vol. 49, No. 3, 467–473, 2007.

6. Sorrentino, A., G. Ferrara, and M. Migliaccio, "On the coherence time control of a continuous mode stirred reverberating chamber," *IEEE Trans. Antennas Propag.*, Vol. 57, No. 10, 3372–3374, 2009.

7. Sorrentino, A., G. Ferrara, and M. Migliaccio, "Comparison between GMSK and PSK modulation systems in the wireless propagation channels emulated in a reverberating chamber," *Proceedings of the 5th European Conference on Antennas and Propagation (EUCAP)*, 1630–1633, 2011.

8. Sorrentino, A., G. Ferrara, and M. Migliaccio, "The reverberating chamber as a line-of-sight wireless channel emulator," *IEEE Trans. Antennas Propag.*, Vol. 56, No. 6, 1825–1830, 2008.

9. Holloway, C. L., D. A. Hill, J. M. Ladbury, P. F. Wilson, G. Koepke, and J. Coder, "On the use of reverberation chamber to simulate a Rician radio environment for testing of wireless device," *IEEE Trans. Antennas Propag.*, Vol. 54, No. 11, 3167–3177, 2006.

10. Chen, X., P. S. Kildal, and S. H. Lai, "Estimation of average Rician K-factor and average mode bandwidth in loaded reverberation chamber," *IEEE Antennas Wireless. Propag. Lett.*, Vol. 10, 1437–1440, 2011.

11. Cappetta, L., M. Feo, V. Fiumara, V. Pierro, and I. M. Pinto, "Electromagnetic chaos in mode — stirred reverberation enclosures," *IEEE Trans. Electromagn. Compat.*, Vol. 40, No. 3, 185–192, 1998.

12. Orjubin, G., E. Richalot, O. Picon, and O. Legrand, "Chaoticity of a reverberation chamber assessed from the analysis of modal distributions obtained by FEM," *IEEE Trans. Electromagn. Compat.*, Vol. 49, No. 4, 762–771, 2007.

13. Haykin, S. and X. B. Li, "Detection of signals in chaos," *IEEE Proc.*, Vol. 83, No. 1, 95–122, 1995.

14. Corona, P., G. Ferrara, and M. Migliaccio, "Generalized stochastic field model for reverberating chamber," *IEEE Trans. Electromagn. Compat.*, Vol. 46, No. 4, 655–660, 2004.

15. Feder, J., *Fractals,* Plenum Press, New York, NY, 1988.

16. Mandelbrot, B. B., *The Fractal Geometry of Nature,* W. H. Freeman and Co., New York, NY, 1982.

17. Baudoin, F. and D. Nualart, "Notes on the two-dimensional fractional Brownian motion," *The Annals of Probability*, Vol. 34, No. 1, 159–180, 2006.

18. Kay, S. M., *Modern Spectral Estimation, Theory and Application*, Prentice Hall, Englewood Cliffs, NJ, 1998.